CO_2 cooling for HEP experiments

B. Verlaat, M. Van Beuzekom, A. Van Lysebetten
Nikhef, Kruislaan 409, 1098 SJ Amsterdam, The Netherlands

bverlaat@nikhef.nl

Abstract

The new generation silicon detectors require more efficient cooling of the front-end electronics and the silicon sensors themselves. To minimize reverse annealing of the silicon sensors the cooling temperatures need to be reduced. Other important requirements of the new generation cooling systems are a reduced mass and a maintenance free operation of the hardware inside the detector.

Evaporative CO_2 cooling systems are ideal for this purpose as they need smaller tubes than conventional systems. The heat transfer capability of evaporative CO_2 is high.

CO_2 is used as cooling fluid for the LHCb-VELO and the AMS-Tracker cooling systems. A special method for the fluid circulation is developed at Nikhef to get a very stable temperature of both detectors without any active components like valves or heaters inside. This method is called 2-phase Accumulator Controlled Loop (2PACL) and is a good candidate technology for the design of the future cooling systems for the Atlas and CMS upgrades.

I. Evaporative CO_2 cooling

In detector applications it is crucial to minimize the hardware needed for the cooling inside the detectors. It is known that two-phase cooling is more efficient than single phase cooling. Less flow is needed and a tube can become almost isothermal when the pressure drop remains low. The smallest diameter evaporator tubes can be achieved with fluids which are evaporating under high pressure. For these fluids, the created vapor can not expand to a large volume. Therefore the pipe volume hence the diameter can stay low. A smaller diameter pipe contains less fluid mass. A high pressure fluid needs a thicker tube wall, but since the pipe diameter is smaller, the increase in mass of the tube wall is compensated by the diameter decrease. Hence, the total mass (tube+fluid) is lower when using a high pressure fluid as compared to a low pressure fluid.

Another good feature of high pressure fluids is that larger pressure drops can be allowed. The influence of the pressure drop is related to the absolute pressure, and therefore less significant for high pressure fluids. This means that even smaller diameter tubes can be used.

Currently used radiation hard fluids are fluor-carbons and CO_2. Figure 1 shows the saturation pressure curves of some these fluids in the temperature range between +10 and -40°C. As can be seen, CO_2 is the best candidate of the three and C_3F_8 the least interesting candidate fluid. A calculation later in this paper will show the superiority of CO_2 compared to the two fluor-carbons.

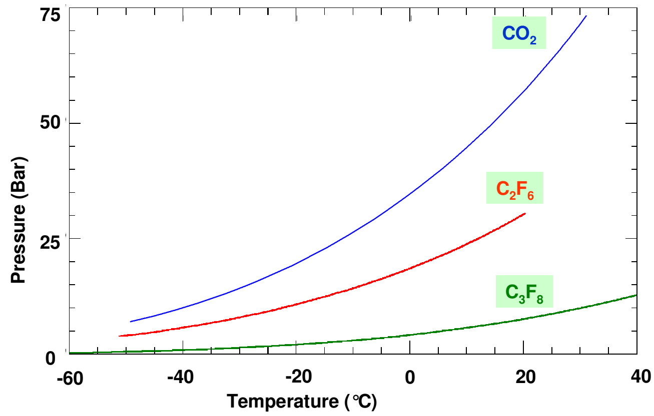

Figure 1: Saturation curves of radiation hard cooling fluids

A. *Temperature distribution in an evaporative cooling tube.*

The pressure along a cooling tube drops in the direction of the flow. This results for two-phase flow in a decrease in temperature due to the decrease of the saturation pressure. In contradictory for single phase flow the temperature increases along the tube due to the heat capacity. Figure 2 shows a typical temperature distribution over a cooling tube with CO_2 starting in single phase at the inlet and ending in gaseous phase at the outlet.

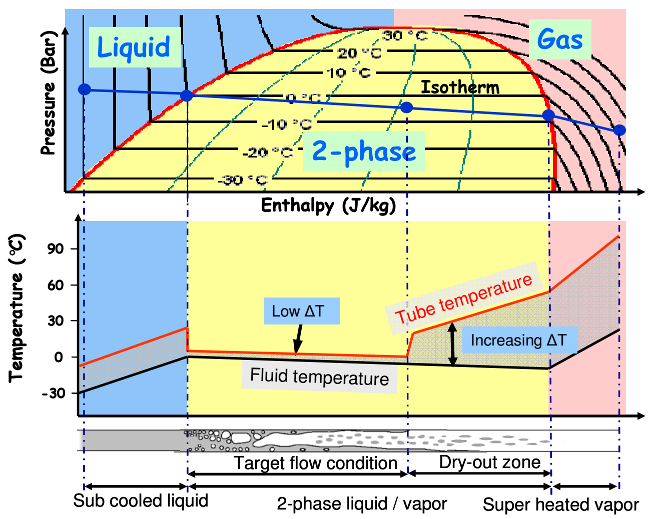

Figure 2: The principle of two-phase cooling versus single phase cooling

At the lower graph the temperature along a tube is shown, with the increasing temperature in the two single phase regions and a decreasing temperature profile in the two-phase region. The black line is the fluid temperature, while the red line is the tube wall temperature. The difference between them is caused by the heat transfer resistance. In the region where the evaporation starts, the heat transfer resistance and hence the temperature difference is low. At a certain vapor quality the heat transfer can get suddenly worse causing a rapidly increasing wall temperature. (Vapor quality is the mass fraction of vapour to liquid in a two-phase flow). The wall temperature increase is due to the fact that the remaining liquid is no longer touching the tube wall which results in a poor heat transfer resistance. This phenomenon is called dry-out.

During a cooling cycle two main parameters change: energy is added or released in the form of enthalpy and pressure is lowered by expansion or increased by pumping or compression. Due to the change of these 2 properties the other important features like the temperature are derived. Setting a temperature directly is not possible; it is achieved by setting the right enthalpy and pressure to achieve the desired temperature. For this reason cooling systems are designed in the pressure-enthalpy diagram of the corresponding fluid. In the top panel of Figure 2 a CO_2 pressure enthalpy diagram shown. The temperature distribution over the tube and the fluid state in the lower panel can be read from this diagram.

B. *Pressure drop and heat transfer*

Two-phase pressure drop as well as two-phase heat transfer is hard to predict accurately as the liquid/vapor flow pattern are very non-uniform. The existing prediction methods are all based on empirical correlations of data fitting in certain operational areas. A lot of research is done on low-pressure fluids in macro tubes, while our applications use high pressure and mini channels. Only a few research results are available for each of these subjects and results on the combination of the two are even harder to find. The calculations in the example in this paper are based on research from several years ago. Although more recent and hence more accurate models have become available in the mean time, it does not influence the comparison of different cooling fluids.

Petterson et al [1] used the Friedel correlation for pressure drop and the Kandlikar correlation for heat transfer during their research of CO_2 in micro channel tubes for automotive air-conditioning in 2000. In both correlations the two-phase formula is the single phase formula multiplied by a correlation factor. An overview of all the relevant equations and parameters are given in chapter VII and VIII. The two-phase pressure drop can be calculated with equation 1:

$$\Delta P_{TP} = \phi_{LO}^{2} * \Delta P_{LO} \qquad (1)$$

ΔP_{LO} is the pressure drop of single phase liquid with the same mass flux. For simplicity the Blasius equation (15,16) can be used. The two-phase pressure drop multiplier can be calculated according to the Friedel correlation:

$$\phi_{LO}^{2} = \frac{E + 3.24 * F * H}{Fr_{TP}^{0.045} * We_{TP}^{0.035}} \qquad (2)$$

The two-phase heat transfer coefficient can be calculated according to the Kandlikar correlation.

$$\alpha_{TP} = \alpha_{LO} * (C_1 * Co^{C_2} * (25 * Fr_{LO})^{C_5} + C_3 * Bo^{C_4} * F_{fl}) \quad (6)$$

α_{LO} is the heat transfer of the of single phase liquid with the same mass flux. For simplicity the Dittus-Boelter equation (7) can be used.

With the above mentioned formulas a possible cooling pipe solution for the upgrade of the Atlas staves (see next section for details) was analysed to give an estimate of achievable tube diameters. An indication of the temperature distribution over the tube for the estimated tube diameter is also given.

C. *Example cooling tube of an Atlas upgrade-stave.*

To demonstrate the superior properties of CO_2 with respect to C_3F_8 and C_2F_6, the cooling of a possible Atlas upgrade stave is analysed for all three fluids. The stave is constructed of two layers of silicon, each layer existing of 20 wafers with a spacing of 10cm. Each wafer assembly dissipates 17 watt. The four meter long cooling tube runs along all wafers and has to absorb a total power of 680 Watt.

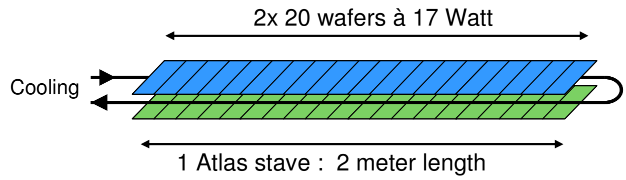

Figure 3: Schematic example of an upgrade Atlas stave

The estimated cooling fluid temperature for this calculation is -35°C and the outlet vapor quality is fixed at 75%. First the pressure drop as a function of the tube diameter is calculated using the pressure drop formula of equation 1. Figure 4 show the pressure drop dependency as a function of the diameter for the three fluids. Figure 5 shows the temperature drop along the tube as a function of diameter. This temperature drop is a result of the changing saturation pressure (temperature drop phenomena explained in figure 2).

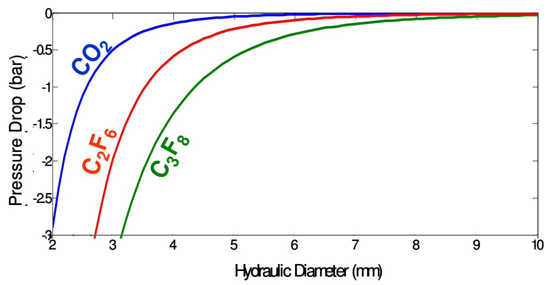

Figure 4: Pressure drop of CO_2, C_3F_8 and C_2F_6 as a function of tube diameter

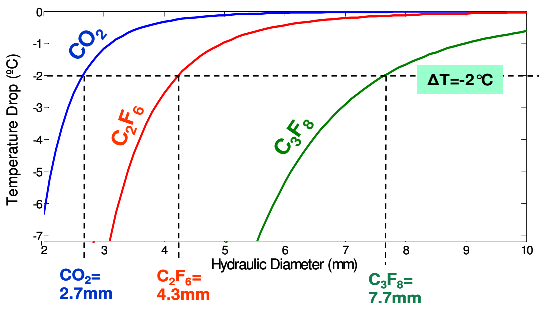

Figure 5: Temperature drop of CO_2, C_3F_8 and C_2F_6 as a function of tube diameter

For a given diameter, the pressure drop of CO_2 is the lowest of the 3, this is due to the high latent heat of CO_2 (less flow=less pressure drop), the low viscosity and the low vapor speed. Table 1 shows the calculated mass flows for the thee fluids at -35°C, 75% exit vapor quality, and 680 Watt. If we assume a maximum temperature gradient over the tube of 2°C we can extract the necessary tube diameters from figure 5. Table 1 shows the tube diameter selection and the corresponding mass flux.

Table 1: Required mass flows, fluxes and diameter

Fluid	Mass flow ($^g/_s$)	Tube diameter (mm)	Mass flux ($^{kg}/_{m^2s}$)
CO_2	2.9	2.7	506
C_2F_6	9.6	4.3	186
C_3F_8	8.7	7.7	661

After selecting the necessary tube diameter the heat transfer to the tube can be calculated. For comparison the heat transfer is calculated over a length of 75mm and 25mm respectively. The heat transfer coefficient is calculated using the Kandlikar correlation as given in equation 3. The fluid dependent parameter F_{fl} is set to 1 for all three fluids assuming stainless steel pipes, as suggested by Kandlikar [2].

Figure 6 shows the calculated heat transfer coefficients. Figure 7 shows the temperature distribution over the cooling tube length for the cooling fluid and the tube wall for both heat exchange lengths. The presented calculation clearly shows the superior behaviour of CO_2 as evaporative cooling fluid for detector applications. A CO_2 evaporator needs the smallest diameter tube and has the best heat transfer coefficients of the three fluids.

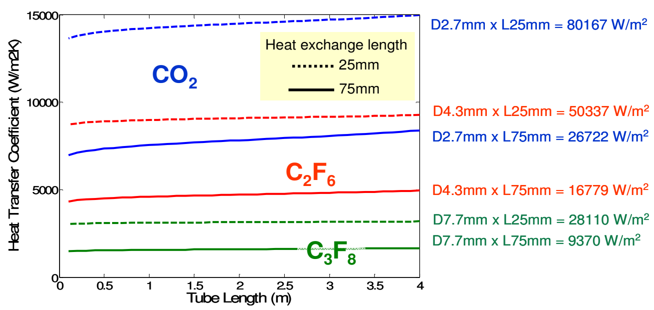

Figure 6: Heat transfer coefficients.

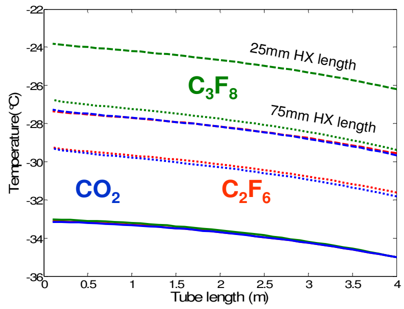

Figure 7: Cooling tube temperature distribution.

D. *Cooling cycle*

After defining a proper two-phase flow in the evaporator tube it is important to select a method to get this two-phase condition in there. In general there are two methods to achieve this. One is a liquid pumped system with an external cold source; the second method is to use the evaporator tube directly in a refrigeration cycle. Both methods have been used at CERN for the LHC experiments. The Atlas inner detector uses a vapor compression system with C_3F_8 as refrigerant [3], The LHCb-VELO Thermal Control System (VTCS) [4,5] uses a liquid pumped system using the two-phase Accumulator Controlled Loop (2PACL) method [6] with CO_2 as working fluid.

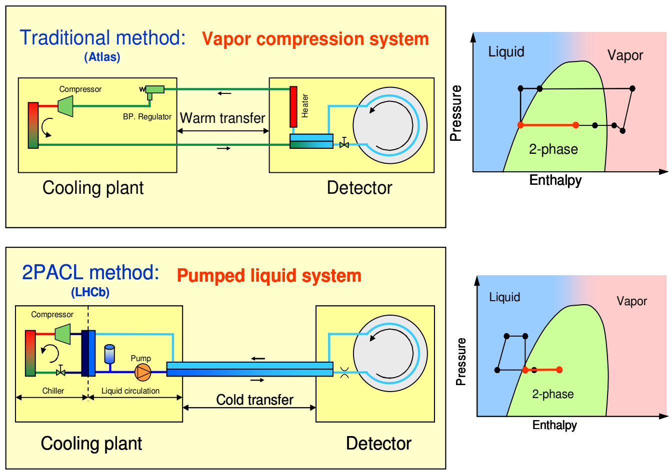

Figure 8: Two-phase cooling system principles used at CERN.

The advantage of the Atlas system is that one can use warm transport lines; a pumped system has cold transfer lines and needs proper insulation. The insulation layer gives extra space requirements, however the tubes are smaller so the mass involved is most likely lower. The disadvantages of the Atlas system are the existence of heaters in the detector to boil-off the remaining liquid, an oil-free compressor is needed as well which is in general harder to find as an oil-free pump. The main advantage of the VTCS-2PACL method is a complete passive evaporator section inside the detector. Neither actuators, nor crucial sensors are needed in the inaccessible detector area.

II. THE 2PACL METHOD

So far two CO_2 cooling systems have been developed for particle physics applications. CO_2 was proposed as alternative cooling fluid for the LHCb-VELO in 1998 [7]. The positive results of the feasibility tests for the LHCb-VELO with CO_2, has inspired the design of Tracker Thermal Control System (TTCS) [8] of the Alpha Magnetic Spectrometer (AMS) for the International Space Station (ISS) [9] to use CO_2 as well. The AMS-TTCS is a mechanically pumped two-phase loop system where the CO_2 vapor is condensed to a cold radiator plate. The evaporator pressure is controlled by a two-phase accumulator which is the regular way of controlling the pressure in a capillary pumped loop. The capillary pumped loop is an evaporative heat transport system where the flow is achieved by capillary pumping. Capillary pumped loops are applied in satellite cooling [10]. The development of a two-phase accumulator in combination with a mechanical pump in the AMS-TTCS, has inspired the design of the LHCb-VELO cooling system. The use of a two-phase accumulator as loop pressure control was named 2PACL method, which stands for two-phase Accumulator Controlled Loop.

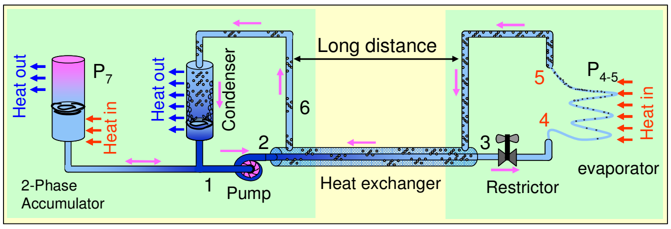

Figure 9: The 2PACL principle

The accumulator vessel is mounted in parallel to the system and contains by design always a mixture of liquid and vapor. This guaranteed presence of a saturated mixture makes the loop pressure to be a function of the accumulator temperature. The 2PACL method works as long as the chiller is able to keep the CO_2 outlet of the condenser colder than the accumulator saturation temperature. In this way the pump is fed with sub-cooled liquid and can run free of cavitation. The internal heat exchanger is heating the sub-cooling, so that the evaporator is always evaporating at the saturation temperature set in the accumulator.

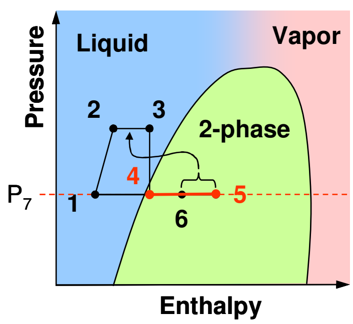

Figure 10: The 2PACL cycle in the Pressure-enthalpy diagram

Figure 10 shows the operation of the 2PACL in the pressure-enthalpy diagram. The nodes in the diagram correspond to the locations in the schematic of figure 9. Node 1 in the liquid zone is the pump inlet, node 2 the pump outlet.

Between node 2 and 3 heat is applied via the internal heat exchanger to reduce sub-cooling. Liquid expansion takes place between node 3 and 4, ending up with saturated liquid at the evaporator inlet. The evaporator is taking up heat from node 4 to 5, where the vapor quality increases due to evaporation. The evaporator outlet (node 5) can still be partly liquid, not all the liquid need to be evaporated as the pump is providing an overflow.

The heat exchanged from node 5 to 6 is equal to the heat applied to node 2 to 3. In the fact of insufficient heat absorption in the evaporator or from the environment, node 6 can be sub-cooled. In this case there is still evaporation in the evaporator but only sub-cooled liquid is present in the condenser. Only at extreme unbalance between the sub-cooling temperature and the evaporator saturation temperature, there is sub-cooled liquid in the evaporator. The 2PACL is now out of its working range. The condenser is the section from node 6 to 1, with sub-cooled liquid supplied back to the pump again at node 1. Nodes 4, 5, 6 and 1 all have the same pressure as the accumulator, neglecting the small pressure drop in the system.

III. THE LHCB VELO DETECTOR

The LHCb-VELO [10] is the sub-detector closest to the collision point in LHCb. It consists of 21 double and 2 single silicon sensor layers which are positioned at about 1 cm distance from the LHC proton beams. The VELO is split into two halves both covering half of the active silicon sensor area. The silicon wafers are mounted on a module containing the read out electronics and mechanical support. The silicon modules are situated in a vacuum volume which is separated only by a 0.3mm aluminium foil from the LHC beam vacuum volume. The maximum allowed pressure difference between the 2 vacuum volumes is 5 mbar, which is controlled by a complex system for pumping down and filling the vacuum volumes simultaneously [12]. The reason for a secondary vacuum is the out gassing of the silicon modules, and the possibility of installing detector hardware without exposing the LHC beam vacuum volume to the air. The 0.3 mm aluminium foil around the silicon modules acts also as a Faraday cage protecting the silicon and electronics from the electromagnetic interference of the proton beams.

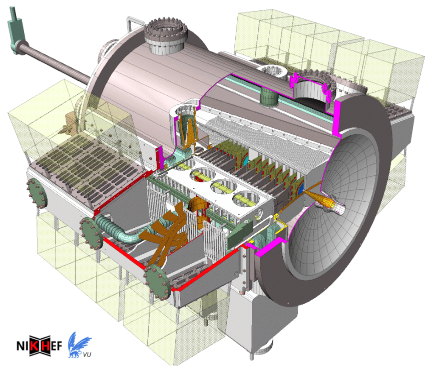

Figure 11: The LHCb-VELO detector with a quarter of the silicon modules visible.

The silicon sensors suffer from a high dose of radiation induced by the LHC proton beams. The radiation causes damage to the silicon crystal lattice resulting in an increase of depletion voltage. Permanent cooling of the sensors is needed to avoid further degradation of the silicon sensors. A silicon temperature less than -7ºC is sufficient to minimize the effects of radiation damage.

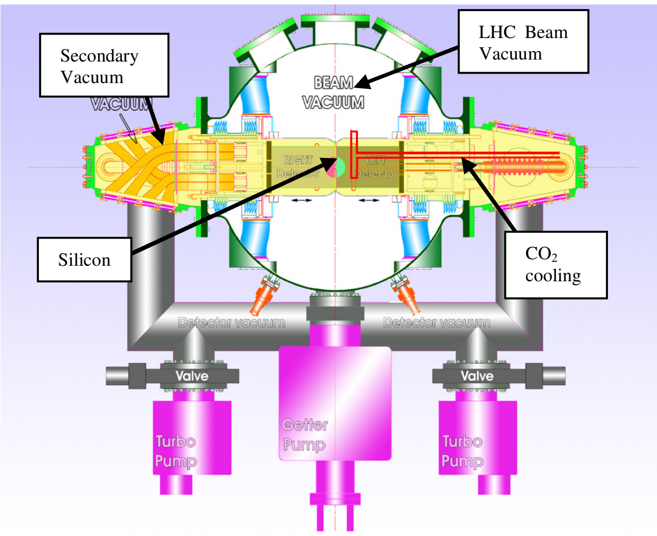

Figure 12: Cross section of the VELO detector

A. VELO module design.

The VELO modules consist of a carbon fiber TPG laminate where on both sides an electronics hybrid with a silicon sensor is glued. At the bottom of this laminate the CO_2 cooling evaporator is mounted on one side and the carbon fiber support paddle on the other side. The paddles are mounted on a stiff aluminium base frame. Figure 13 shows a picture of an assembled VELO half with the discussed items clearly visible. The Beetle read-out chips are located on the hybrid at the edge of the silicon and can generate up to 28 watts of heat per module which needs to be taken away by the CO_2 cooling system. The aluminium base is the positional reference of the modules and must stay at room temperature. This is achieved by heaters since the thermal connection via the paddles to the CO_2 evaporators will otherwise cause the base to cool down.

Figure 13: Assembled VELO half with silicon modules, cooling blocks, and module base

B. CO_2 evaporator design.

Each silicon module is connected to a dedicated parallel evaporator branch. Each branch consists of a 1 meter long stainless steel capillary of 1.5x0.25mm, which is embedded in an aluminium cooling block which is attached to the carbon fiber/TPG laminate. The aluminium cooling block is obtained with a casting procedure specially developed at Nikhef. The Aluminium is melted around the tube in a vacuum oven, so that the Al joins the stainless steel in a chemical way. The casting will give a lot of freedom in pipe geometry inside the aluminium and a perfect thermal contact between the pipe and the cooling block. Each evaporator branch has a 1.3 meter restriction capillary of 1x0.2 mm at the inlet to obtain a good flow distribution over all the evaporator branches. The presence of the evaporator in a vacuum system gives high constraints to the leak tightness. Therefore the complete evaporator assembly (figure 14) is made of stainless steel tubes all joined together with vacuum brazing or orbital welding. No connectors are present inside the vacuum system. The inlet manifold connected to the inlet capillaries is outside the vacuum vessel and is accessible. This way it is possible to connect cooling to individual channels, a feature which is used by module commissioning using a small scale test cooling system.

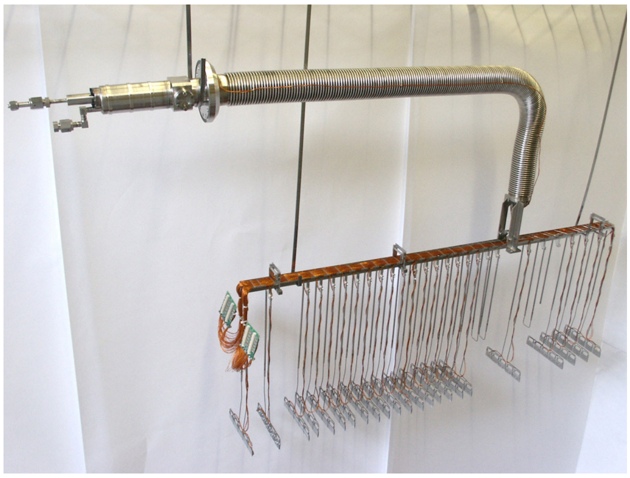

Figure 14: VTCS CO_2 evaporator assembly

IV. The VELO Thermal Control System (VTCS).

The VTCS is a cascade of three hydraulic systems. A Freon chiller condenses the CO_2 vapor and rejects the waste heat to the cold water system of CERN. This chiller has a gas compressor, water condenser, evaporators and expansion valves. The water system is called the primary cooling system, the chiller the secondary and the CO_2 loop the tertiary cooling system. Figure 15 shows a schematic diagram of the cascade systems, with the main heat flows and the system temperature distribution.

The VTCS also has an air-cooled chiller with lower capacity. This back-up can only cool the CO_2 loops to -10°C and has no capacity left over to absorb detector power. It is only for maintaining the unpowered detector cold to avoid radiation damage in case of a problem or during maintenance.

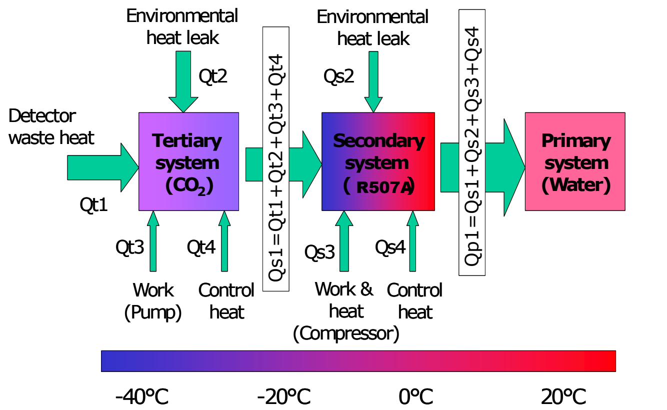

Figure 15: Block diagram and heat balance representation of the VTCS

The cooling plant of the VTCS is placed 55 m away from the VELO detector behind a thick concrete shielding wall (See figure 16). This wall shields the system from the radiation of the LHC. The VTCS is designed such that all active hardware is located in this safe zone. The cooling hardware in the experimental area consists only of tubes and passive devices such as restrictors and one-way valves. Sensors (pressure and temperature) in the radiation zone are only for monitoring and are not important for the cooling system operation.

The CO_2 evaporators in the detector are connected to the VTCS via 55 meter long concentric transfer lines. The liquid feed transfer tube (1/4"x0.035") is situated inside the vapor return tube (16mm x 1mm). The concentric construction acts as a long counter flow heat exchanger needed for conditioning the evaporator inlet flow to be saturated.

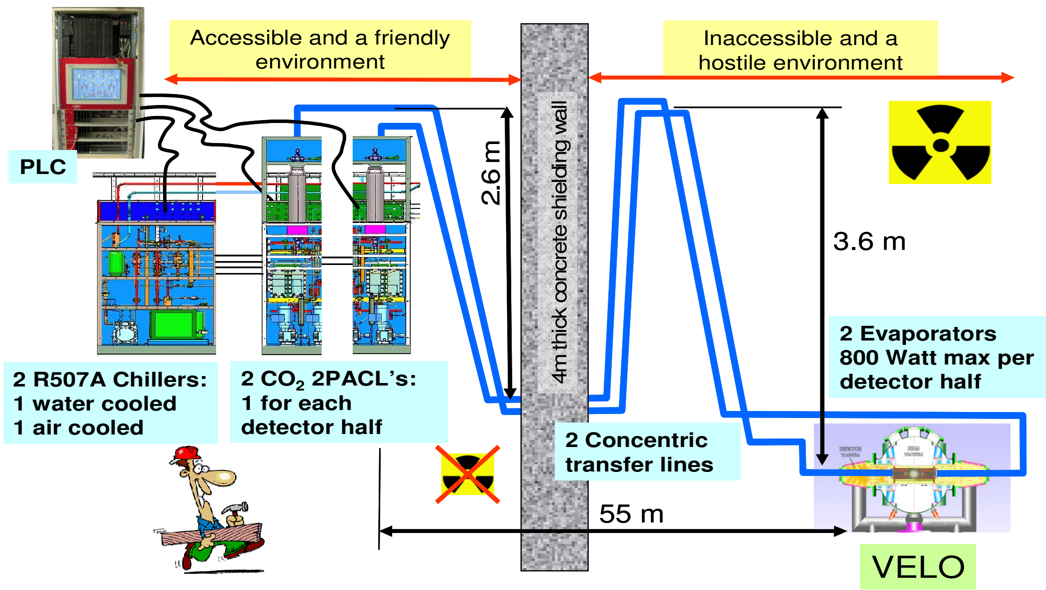

Figure 16: VTCS set-up in the LHCb cavern

The flow in the evaporator must be of low vapor quality to achieve a stable liquid expansion in the flow distribution capillaries. The needed evaporator temperature to achieve the silicon temperature requirement is between -25°C and -30°C [13]. This temperature can be set in the system by controlling the accumulator pressure and hence saturation temperature. This temperature setting of the accumulator is called the VTCS set-point. For commissioning the set-point can be set higher, as the silicon sensors are not yet irradiated. Under vacuum the cooling temperature for commissioning is -5°C, for commissioning under Neon atmosphere the cooling temperature is +10°C. Operating the cooling at +10°C is achieved by using the back-up air-cooled chiller, as the water cooled chiller is to powerful for operation at higher temperatures than -5°C.

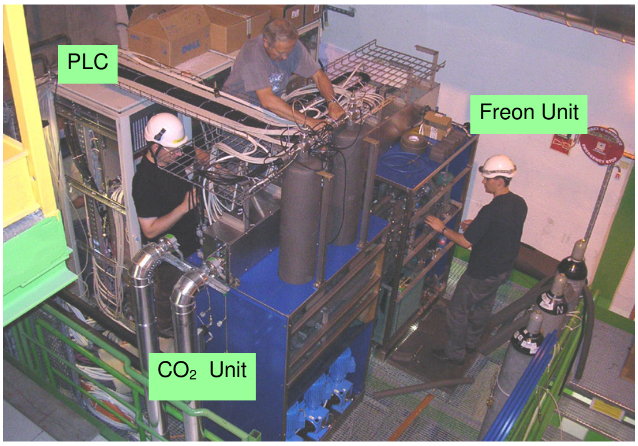

Figure 17: The VTCS cooling plant in the LHCb-cavern

The cooling system is controlled by a Siemens S7-400 series Programmable Logic Controller (PLC). It controls the two independent CO_2 loops and also the water cooled main chiller and air cooled backup chiller. Moreover, the PLC handles all the VTCS safety alarms and it interlocks to other subsystems of the VELO like low voltage, bias voltage and vacuum system. In total the cooling system contains about 20 pressure sensors, more than 150 temperature sensors and over 20 actuators such as pumps, valves, compressors and heaters. Note that only a fraction of these sensors are crucial for the operation of the cooling system. The other sensors allow us to study the behaviour of the system in great detail. This is important as the VTCS is the first CO_2 based cooling system in use at a HEP experiment. The main control task in the CO_2 loops is to regulate the pressure by either evaporating liquid or by condensing vapor in the accumulator. Stabilisation is achieved by PID loops. For the freon chillers the most important tasks are the control of the expansion valves for the CO_2-freon heat exchangers and the frequency of the compressor.

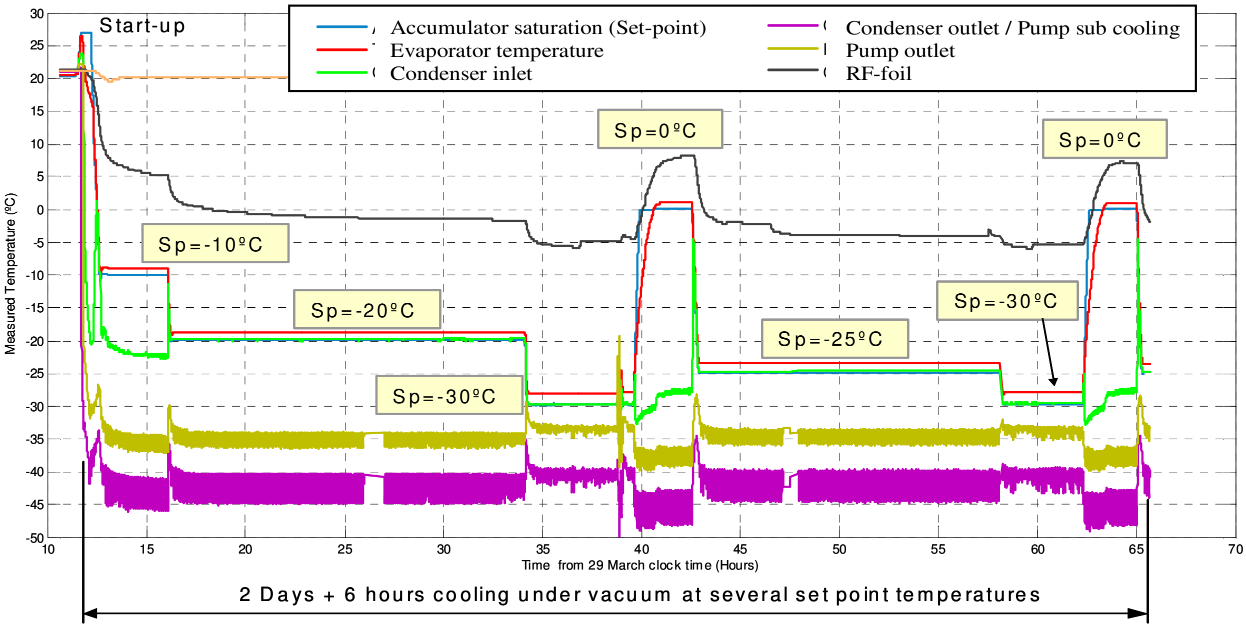

Figure 18: Unpowered detector cooling tests under vacuum in March 2008.

V. COMMISSIONING RESULTS OF THE VTCS.

The VTCS was installed in 2007 and commissioning was started early 2008. The full detector was not operational until May 2008. Prior to detector availability, dummy heaters were installed near the VELO to replace the detector heat load. The flow through the detector was by-passed, as it was not allowed to cool the detector below 10°C under Neon vented condition of the vacuum volumes. The VTCS was tested using the dummy heaters under several heat loads up to 800 Watt per loop.

In March 2008 the detector was for the first time cooled under vacuum conditions at several operational temperatures ranging from 0°C to -30°C (See figure 18). There was no power dissipated neither in the detector nor in the dummy heaters. The detector electronics were not yet cabled.

In May the detector was powered on module by module under Neon atmosphere with the back-up chiller at 10°C cooling only one detector half. After the successful detector powering tests, the detector was evacuated to vacuum at the end of June for upcoming LHC commissioning. Following the evacuation the full detector was commissioned with its designed cooling temperature of -25°C and all the electronics switched on.

The start-up of the left VTCS is shown in figure 19. Around 13.4 clock time the accumulator started heating (7,red) to increase the pressure (7,gold) to 27°C saturation temperature. As the loop saturation temperature is higher than the environment temperature, the loop is filled with liquid and consequently the accumulator liquid level is dropping (7,blue). Around 13.6 hour the pump was started as can be seen by the increase of the pump head pressure (2). The chiller is started right after this cooling down the liquid flow to the pump (1). After pumping cold liquid for a while, the accumulator is cooled to bring the pressure down to the desired set-point pressure and hence temperature. The accumulator cooling is the negative signal from the combined heating/cooling control (7, red). Due to the accumulator cooling, the accumulator is filling as can be seen by the increasing liquid level (7,blue). Around 14.7 hour the set-point has been reached and the temperatures and pressures stay constant. The accumulator remains to be cooled to compensate the environmental heat leak from the environment. The VTCS is now ready for detector power.

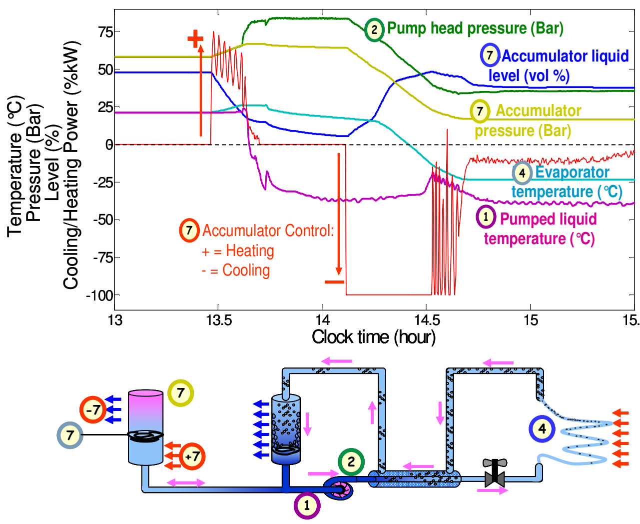

Figure 19: Start-up of the left-VTCS 2PACL

Figure 20 shows the powering-up of the left detector with the cooling set-point to be -25°C. Around 15 minutes the detector is switched on. The purple line is the individual heat load of one module, the blue line the total heat load of the left detector. As a result the module temperature (black line) and the silicon temperature (green line) are increasing. The silicon is stabilizing around -7°C; this is according to the design requirements. The applied heat in the evaporator increases the amount of vapour in the system which causes the pressure and hence the evaporator temperature to rise a bit. The accumulator control is reacting to this pressure offset by cooling the accumulator (cyan line). As a result is the liquid level (red line) increases because the generated amount of vapor is accumulated in the accumulator. After a small deviation the evaporator temperature is maintained.

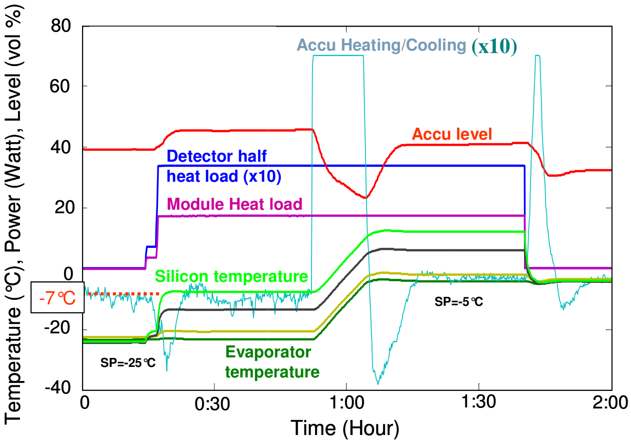

Figure 20: Commissioning results of the Left VELO detector cooling.

After running stabile with the detector being powered, the set-point temperature was changed to -5°C. Around 50 minutes the accumulator control reacts with heating the accumulator (cyan line) and hence a decreasing liquid level (red line). The temperatures of the evaporator and the module are increasing until the -5°C set-point is reached. The accumulator control stops heating and stabilizes with a small cooling action. Around 1:40, the detector is powered down, and the VTCS is reacting to the opposite way compared to the detector powering up. The accumulator is heated and the liquid level is dropping, because the amount vapour in the loop is decreasing.

VI. Conclusions and Outlook.

This paper has demonstrated that CO_2 as evaporative coolant is very promising. It has multiple advantages for detector applications as CO_2 seems to add less mass to the detector compared to evaporative cooling with fluor-carbons. The possibility of using smaller tubing is not only beneficial for the mass budget, but gives also more flexibility in the design as the pipes are more flexible. Flexible tubing gives less structural impact on the detector mechanics, such as thermal expansion.

The 2PACL method was presented in this paper. The VTCS was built according to this principle and the VTCS works as expected. The requirements are met, as the silicon was operating at -7°C at the designed cooling temperature of -25°C. The evaporator temperature turned out to be very stable; fluctuations of less than 0.05 °C were measured over time. The VTCS set-point range was determent to be between -5°C and -30°C.

The construction of the VTCS is not yet finished. The VTCS commissioning has learned us that an accumulator connection at the inlet of the condenser is working better than the location after the condenser were it is now. The accumulator heating was sometimes giving saturated liquid to the pump, causing the pump to cavitate. The accumulator connection swap will solve this problem. One 2PACL side (right system) was temporarily modified, and results were promising. It was decided to implement this modification on both 2PACLs. These modifications will be done early 2009. Other ongoing works are the implementation of the automatic back-up procedures, the chiller expansion valve tuning and the integration of the system in the PVSS-finite state machine.

VII. Nomenclature

ΔP = Pressure drop (Bar)

ϕ^2 =two-phase pressure drop multiplier

E, F, H = Friedel correlation constants

α = Heat transfer coeeficient (W/m^{2}K)

Fr = Froude number

We = Weber number

Re =Reynolds number

Pr = Prandl number

Co = Convection number

Bo = Boiling number

Nu = Nusselt number

h = Enthalpy (J/kg)

λ = Thermal conductivity (W/mK)

ρ = Density (kg/m^3)

η = Dynamic viscosity (Pa*s)

σ = Surface tension (N/m)

Cp=Heat capacity (J/kg*K)

x= Vapor quality

g = Specific gravity (m/s^2)

f = Friction factor

m'= Mass flux (kg/m*s^2)

q' = Heat flux (W/m^2)

D = Hydraulic diameter (m)

C_1 = Kandlikar's nucleate boiling constant: 0.6683

C_2= Kandlikar's nucleate boiling constant: -0.2

C_3= Kandlikar's nucleate boiling constant: 1058

C_4= Kandlikar's constant: 0.7

C_5= Kandlikar's constant: 0 (Fr_{LO}>0.04), 0.3 (Fr_{LO}<0.04).

F_{fl} = Fluid surface parameter: 1 for stainless steel tubes

Indices:

TP =Two Phase

LO = Liquid only

L =Liquid

G =Vapor

VIII. EQUATIONS:

(1) $\Delta P_{TP} = \varphi_{LO}^{2} * \Delta P_{LO}$

(2) $\varphi_{LO}^{2} = \dfrac{E+3.24*F*H}{Fr_{LO}^{0.045} * We_{LO}^{0.035}}$

(3) $E = (1-x)^2 + x^2 \left(\dfrac{\rho_L * f_{GO}}{\rho_G * f_{LO}}\right)$

(4) $F = x^{0.78} * (1-x)^{0.24}$

(5) $H = \left(\dfrac{\rho_L}{\rho_G}\right)^{0.91} * \left(\dfrac{\eta_G}{\eta_L}\right)^{0.19} * \left(1-\dfrac{\eta_G}{\eta_L}\right)^{0.7}$

(6) $\alpha_{TP} = \alpha_{LO} * (C_1 * Co^{C_2} * (25 * Fr_{LO})^{C_5} + C_3 * Bo^{C_4} * F_{fl})$

(7) $\alpha_L = Nu * \lambda_L / D$

(8) $Fr = \dfrac{\dot{m}^2}{g*D*\rho^2}$

(9) $We = \dfrac{\dot{m}^2 * D}{\rho_{TP} * \sigma}$

(10) $Re = \dfrac{\dot{m}^2 * D}{\eta}$

(11) $Pr = \dfrac{\eta_L * Cp_L}{\lambda_L}$

(12) $Co = \left[\dfrac{1-x}{x}\right]^{0.8} * \left[\dfrac{\rho_G}{\rho_L}\right]^{0.5}$

(13) $Bo = \dfrac{\dot{q}}{\dot{m} * (h_G - h_L)}$

(14) $Nu = 0.023 * Re^{0.8} * Pr^{0.4}$

(15) $\Delta P_L = \dfrac{2 * f_L * \dot{m}^2}{D * \rho_L}$

(16) $f_{LO} = \dfrac{0.079}{\sqrt[4]{Re_{LO}}}$

IX. REFERENCES

[1] Pettersen, J., Rieberer, R., Munkejord, S.T.,2000, “Heat Transfer and Pressure Drop for Flow of Supercritical and Subcritical CO_2 in Microchannel Tubes”, Norwegian University of Science and Technology/SINTEF Energy Research, TR A5127

[2] Kandlikar S et al, 2005, “Heat Transfer and Fluid Flow in Minichannels and Microchannels”,ISBN:0-0804-4527-6

[3] Attree D. et al, 2008, “The evaporative cooling system for the ATLAS inner detector”, 2008 Jinst 3 P07003.

[4] Verlaat B. et al, 2008,” CO_2 cooling for the LHCb-VELO experiment AT CERN”, 8th IIF/IIR Gustav Lorentzen Conference on Natural Working Fluids 2008, Copenhagen, Denmark, CDP 16-T3-08

[5] M. Van Beuzekom, A. Van Lysebetten, B. Verlaat 2007, “CO_2 cooling experience (LHCb)”, The 16th International Workshop on Vertex detectors, Lake Placid, NY, USA, PoS 009

[6] Verlaat B., 2007, Controlling a two-phase CO_2 loop using a two-phase accumulator, International Conference of Refrigeration 2007, Beijing, China, ICR07-B2-1565

[7] Boer Rookhuizen H. et al, 1999, “Preliminary Studies for the LHCb Vertex Detector Cooling System”, LHCb note, 99-046/VELO

[8] Verlaat, B., Woering, A., Pauw, A., Delil, A.A.M., 2003, “AMS-2 Tracker Thermal Control System: design and thermal modeling of the mechanically pumped two-phase CO_2 loop”, AIAA Aerospace Sciences Meeting & Exhibit, Reno, NV, USA, AIAA-2003-0345

[9] Borgia, B, 2005, “The Alpha Magnetic Spectrometer on the International Space Station”, IEEE Transactions on Nuclear Science, Vol. 52, No. 6, p. 2786-2792

[10] Delil, A.A.M. et al., 1997, “In-orbit demonstration of two-phase heat transport technology - TPX II reflight”, European Space Agency, SP-400, p.355

[11] LHCb Coll., 2001, “The LHCb VELO technical design report”, CERN/LHCC 2001-0011

[12] Van Beuzekom M. et al, 2008, “The LHCb VELO Vacuum System User manual”, CERN EDMS 901535.

[13] Verlaat, B, 2005, “Thermal performance testing of the VTCS evaporator and VELO module”, NIKHEF EN05-01